AGU PUBLICATIONS

Geophysical Research Letters

RESEARCH LETTER
10.1002/2014GL061535

Key Points:
- Monthly EVI anomalies are not sensitive to radiation or rainfall extremes
- EVI seasonality in the Amazon is still present after BRDF correction
- Although EVI and GPP correlate, interpretations of causality require caution

Supporting Information:
- Readme
- Text S1

Correspondence to:
E. E. Maeda,
eduardo.maeda@helsinki.fi

Citation:
Maeda, E. E., J. Heiskanen, L. E. O. C. Aragão, and J. Rinne (2014), Can MODIS EVI monitor ecosystem productivity in the Amazon rainforest?, *Geophys. Res. Lett.*, *41*, doi:10.1002/2014GL061535.

Received 14 AUG 2014
Accepted 30 SEP 2014
Accepted article online 2 OCT 2014

Can MODIS EVI monitor ecosystem productivity in the Amazon rainforest?

Eduardo Eiji Maeda[1], Janne Heiskanen[1], Luiz E. O. C. Aragão[2], and Janne Rinne[1]

[1]Department of Geosciences and Geography, University of Helsinki, Helsinki, Finland, [2]National Institute for Space Research, São José dos Campos, Brazil

Abstract The enhanced vegetation index (EVI) obtained from satellite imagery has often been used as a proxy of vegetation functioning and productivity in the Amazon rainforest. However, recent studies indicate that EVI patterns are strongly affected by satellite data artifacts. Hence, it is unclear if EVI is sensitive to subtle seasonal variations in evergreen Amazon forest productivity. This study analyzes 12 years of Moderate Resolution Imaging Spectroradiometer (MODIS) EVI in order to evaluate its response to factors driving productivity in the Amazon. We show that, after removing cloud and aerosol contamination, and correcting bidirectional reflectance distribution function effects, radiation and rainfall extremes show no influence on EVI anomalies. However, EVI seasonal patterns are still evident after accounting for Sun-sensor geometry effects. This remaining pattern cannot be explained by solar radiation or rainfall, but it is significantly correlated to gross primary production (GPP). Nevertheless, we argue that the causality between GPP and EVI should be interpreted with caution.

1. Introduction

The impacts of climate variability on the Amazon forest are still under debate. In particular, understanding the effects of climate extremes on the Amazon ecosystem remains scientifically challenging [*Samanta et al.*, 2012a; *Asner and Alencar*, 2010; *Aragão et al.*, 2014]. Recent studies have shown that long periods of water stress have the potential of triggering the release of massive amounts of carbon to the atmosphere [*Lewis et al.*, 2011] by causing widespread tree mortality [*Phillips et al.*, 2010].

Remote sensing has been broadly considered an essential tool for monitoring the Amazon ecosystem [*Anderson et al.*, 2010; *Asner and Alencar*, 2010; *Silva et al.*, 2013]. For instance, vegetation indices (VI) obtained from satellite observations are often used as a proxy for assessing vegetation functioning and net primary production [e.g., *Myneni et al.*, 2007; *Samanta et al.*, 2012b]. Hence, changes in VI patterns are considered as an indicator of the forest response to external environmental factors, such as water availability and solar radiation [*Bradley et al.*, 2011; *Brando et al.*, 2010].

Controversial studies on the Amazon forest response to climate variability have been reported in recent years. Using enhanced vegetation index (EVI) obtained from the Moderate Resolution Imaging Spectroradiometer (MODIS), *Huete et al.* [2006] showed an increase in EVI during the dry season, contradicting model predictions that water limitation would lead to declines in forest greenness. Similarly, *Saleska et al.* [2007] reported that EVI data indicated an excessive greening of the Amazon forest during a strong drought in 2005. Nevertheless, using an EVI data set with improved cloud and aerosol removal, *Samanta et al.* [2010] found no correlation between drought severity and greenness in intact Amazon forests during the 2005 drought. Similar studies analyzed the drought in 2010 and reported a severe and persistent decline in vegetation greenness in 51% of all drought-stricken forests [*Xu et al.*, 2011].

In most cases, discussions aiming to understand these heterogeneities in EVI patterns have focused on the hypothesis that in the Amazon forest radiation supersede water limitation inducing enhancement of EVI values during dry or drought conditions. However, the hypothesis that the EVI patterns in Amazon forest are driven by radiation has recently been undermined as *Morton et al.* [2014] showed that greening did not take place during the dry season. Confirming evidences reported by *Moura et al.* [2012] and *Galvão et al.* [2011], *Morton et al.* [2014] demonstrated that artifacts associated with MODIS Sun-sensor geometry are the primary cause for the greening observed during the dry season. Against the backdrop of this new evidence, it is currently unclear whether changes in vegetation functioning caused by climate variability can be captured

using satellite EVI. Therefore, uncertainties in terrestrial ecosystem models based on VIs are high, and the reliability of model estimates of vegetation productivity under question, as the sensitivity of models to artifacts in remote sensing data still need to be formally evaluated.

In this study, we performed a sensitivity analysis to quantify the response of MODIS EVI to radiation and rainfall extremes throughout the year. Furthermore, the sensitivity of EVI anomalies to changes in Sun-sensor geometry was evaluated. Finally, we tested the hypothesis that EVI can be used as a proxy to describe gross primary production (GPP) and evaluated how environmental factors affect the relationship between EVI and GPP.

2. Materials and Methods

To comprehensively assess EVI sensitivity to climate and Sun-sensor geometry, as well as to test the coherence between EVI signal and GPP, we performed a set of analyses at multiple spatial and temporal scales. A hierarchical approach was adopted to clearly distinguish data artifacts from environmental factors that influence the EVI signal. This was done by using four levels of EVI data, based on their quality and level of correction performed, as described below.

Two EVI data sets were derived from the MODIS MOD13A2 product. The first data set (EVI_M) was created by calculating monthly EVI as an average of 16 day composite images inside a month. In this case, only a superficial quality screening was performed (see supporting information). The second data set followed the same procedure, but this time more strict quality assessment (QA) criteria were used to remove pixels contaminated with clouds, aerosols, and shadows. This data set is hereafter denominated EVI_{QA}.

The third EVI data set was compiled using the blue, red, and near-infrared (NIR) reflectance from the MCD43B4 product. The MCD43B4 provides bidirectional reflectance distribution function (BRDF) model adjusted nadir view reflectance data for 16 day periods at 1 km spatial resolution. The solar zenith angle corresponds to the angle at local solar noon. This data set is hereafter denominated EVI_{NBAR} (Nadir BRDF Adjusted Reflectance).

The fourth EVI data set was compiled using the MCD43B1 product, which contains MODIS BRDF model weights used to derive the NBAR product. However, for this later data set, the Sun zenith angle was fixed to 30° for all months of the year. We refer to this data set as EVI_{SAR} (Sun angle Adjusted Reflectance).

Monthly values of surface downward shortwave radiation flux were obtained from the Clouds and the Earth's Radiant Energy System SYN1deg product. Monthly rainfall values were obtained from the Tropical Rainfall Measuring Mission (TRMM). The phase angle (i.e., the angle between the directions of Sun illumination and sensor view) was calculated using the solar zenith angle, view zenith angle, and relative azimuth angle provided in the MOD13A2 product.

First, we assessed the sensitivity of monthly EVI anomalies to changes in radiation and rainfall within the entire extent of the Amazon basin. For the EVI_{QA} data set, which does not assume fixed observation geometry, we also evaluated how changes in phase angle are linked to VI anomalies.

Monthly standardized anomalies, for all data sets, were calculated using as baseline the period between 2001 and 2012. The sensitivity analyses consisted in grouping EVI anomaly pixels within bins of radiation anomalies, rainfall anomalies, or phase angle. The distributions of EVI anomalies were then constructed within each bin, and the bins median was computed. For radiation and rainfall anomalies, the bin width used was 0.5σ, ranging from -2.5 to 2.5σ. For phase angle the bins width was 5°, ranging from 10 to 60°. An illustration of this approach is provided in Figure S2 in the supporting information.

Next, the influence of external factors on EVI_{SAR} seasonality was studied at the Jurua River watershed, which was chosen for having homogeneous and relatively intact forests. Finally, after clarifying the influence of environmental factors and data artifacts on all EVI data sets, we evaluated the relationship between monthly EVI_{SAR} values and gross primary production (GPP) estimated by eddy covariance at a primary rainforest at KM67, south of Santarém in at the Tapajós National Forest (54°58'W, 2°51'S) [*Hutyra et al.*, 2007]. The relationship was assessed at monthly time scale using records from January 2002 to January 2006. In addition, long-term averages of net ecosystem exchange (NEE), ecosystem respiration (R_{eco}) [*Hutyra et al.*, 2007], and leaf litterfall [*Rice et al.*, 2008] at the flux tower location were analyzed. EVI_{SAR} values were obtained as an average of all valid pixels inside a circular area of 5 km radius around the tower location.

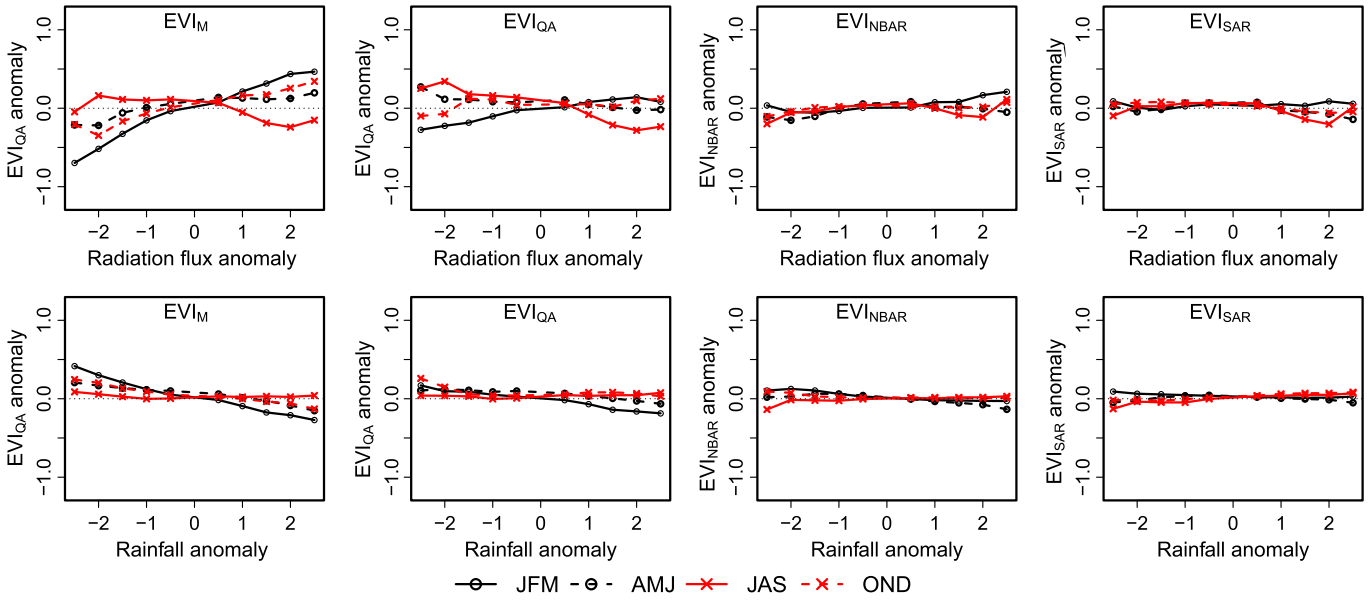

Figure 1. Relationships of EVI and shortwave radiation flux anomalies, for quarters of the year, using the EVI_M, EVI_{QA}, EVI_{NBAR}, and EVI_{SAR} data sets. The lines indicate the median of EVI anomaly values in each radiation anomaly bin of 0.5σ in width. JFM, January-February-March; AMJ, April-May-June; JAS, July-August-September; OND, October-November-December.

3. Results and Discussion

The relationships between EVI and radiation flux anomalies for the entire Amazon basin are presented in Figure 1. When using the EVI_M data set, positive trends are observed during the first, second, and fourth quarters of the year. In the EVI_{QA} data set, the trends during the second and fourth quarters disappear. However, during the first quarter, a positive slope is still observed, while an inverse relationship is observed during the third quarters. Hence, although cloud and aerosol interference are in fact responsible for creating unrealistic association between EVI and radiation anomalies, trends are still observed after strict data quality control in the MOD13 product.

During the first quarter (JFM), cloud interference affects the relationship by creating a steeper curve between EVI_M and radiation. Lower radiation anomalies are associated with a more stable cloud cover, which increases reflectance in the red band in relation to reflectance in the near infrared, reducing the EVI_M values.

In the analysis using EVI_{NBAR} and EVI_{SAR} data sets, no significant relationships are observed, in any season of the year. These results indicate that the trends observed using the EVI_{QA} data set are likely associated with BRDF effects or residual cloud contamination. Hence, after accounting for cloud, aerosol, and BRDF effects, we find no evidences that variations in incoming solar radiation have influence on EVI_{SAR} anomalies in the Amazon basin.

Similar results are also observed in the relationship between the EVI and rainfall anomalies (Figure 1). Considering the EVI_M data set, a decrease in EVI anomalies is observed with increasing rainfall anomalies (first, second, and third quarters). However, this pattern fades when using the EVI_{QA} data set and virtually disappears when considering the EVI_{NBAR} and EVI_{SAR} data sets. These results show that the decrease in water input during meteorological droughts has no impact on the Amazon forest greenness. Although these evidences challenge previous claims that EVI anomalies are affected by droughts [e.g., *Brando et al.*, 2010; *Saleska et al.*, 2007], it cannot discard the hypothesis that the photosynthetic capacity of the forest is water limited, given the possibility that EVI may not be sensitive enough to capture sudden changes in canopy structure and/or chemical composition caused by water stress.

The response of vegetation greenness to radiation anomalies shows similar results throughout different geographical regions of the Amazon basin. The sensitivity of EVI_{SAR} to variations in radiation anomalies, analyzed in four quadrants of the Amazon basin, is presented in Figure S5 (supporting information). Although a slightly larger variance in EVI_{SAR} anomalies is observed in the SE quadrant of the basin, no evident trends are observed between medians of EVI_{SAR} anomalies and radiation anomaly flux bins.

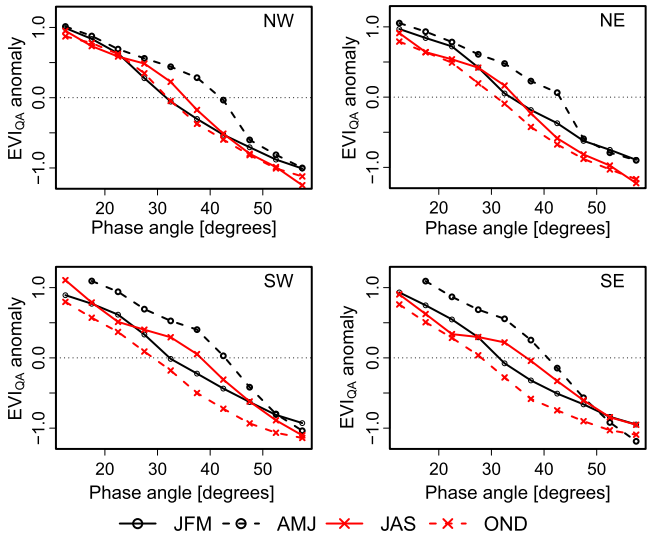

Figure 2. Relationships of EVI_{QA} and phase angle in the Amazon basin, divided in four quadrants. The lines indicate the median of EVI anomaly values in each radiation anomaly bin of 5° in width.

Contrasting with the results obtained using climatic variables, EVI_{QA} anomalies show a consistent response to changes in Sun-sensor geometry (Figure 2). Lower phase angles (i.e., between 10 and 25°) are associated with positive EVI_{QA} anomalies, while higher-phase angles associated to negative EVI_{QA} anomalies. This result is consistent in every season of the year and geographical region. These results provide solid evidence that the spatial and temporal distributions of EVI anomalies obtained using the MOD13 products are largely associated with variation in Sun-sensor geometry.

Hence, it is demonstrated that anomalies in the EVI_M and EVI_{QA} data sets are closely associated with cloud contamination and, particularly, Sun-sensor geometry. On the other hand, when analyzing EVI data sets accounting for BRDF effects (EVI_{NBAR} and EVI_{SAR}), anomalies cannot be explained by variations in incoming solar radiation or rainfall. However, after clarifying the main factors affecting greenness anomalies, a remaining question is how environmental factors affect EVI seasonal patterns of Amazonian forests.

To address this question, we evaluate monthly long-term averages (2001–2012) of EVI_{NBAR}, EVI_{SAR}, radiation, rainfall, and phase angle for the upper Jurua River basin (Figure 3). This assessment was performed in a smaller and homogeneous area to avoid misinterpretations associated with spatial variations in climate and

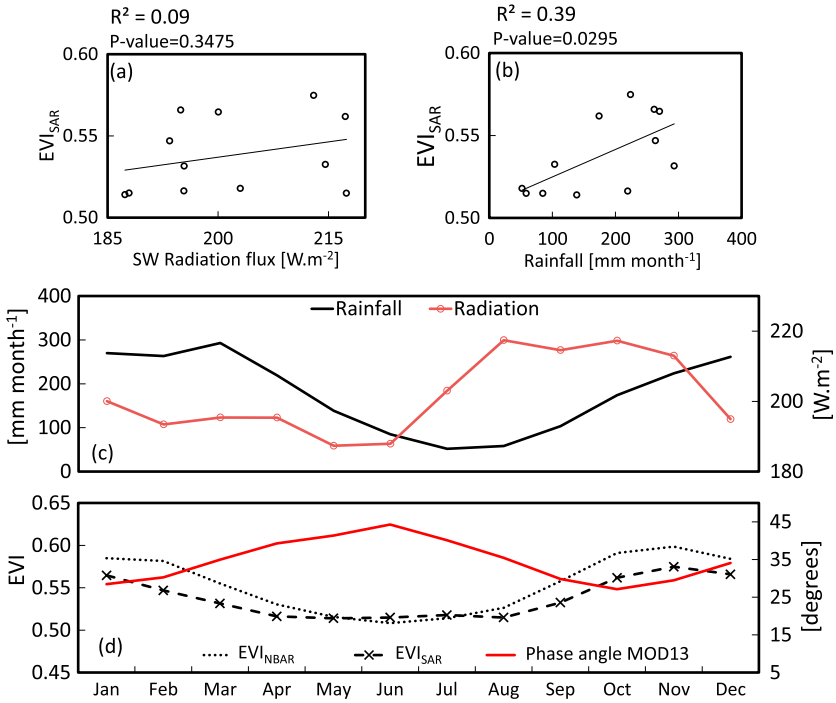

Figure 3. (a) Relationship between monthly EVI_{SAR} and incoming shortwave radiation flux; (b) relationship between monthly EVI_{SAR} and rainfall; (c) long-term (2001–2012) monthly averages of radiation and rainfall; and (d) long-term (2001–2012) monthly averages of EVI_{NBAR}, EVI_{SAR}, and phase angle obtained for the upper Jurua River basin.

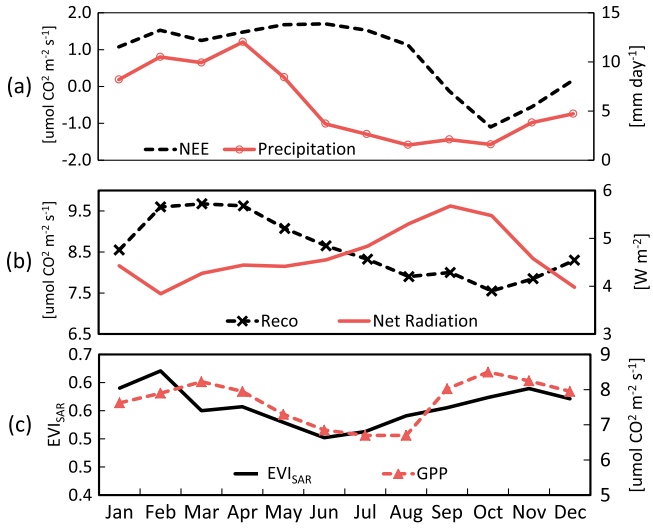

Figure 4. (a) Monthly average net ecosystem exchange of CO_2 (NEE) and rainfall; (b) monthly average ecosystem respiration (Reco) and net radiation; (c) monthly average gross ecosystem production (GPP) and EVI_{SAR} (with BRDF correction with constant Sun zenith angle) for the location of the K67 Eddy Covariance tower. Records are from January 2002 to January 2006 [*Hutyra et al.*, 2007].

vegetation. Only pixels with at least 5 years of valid data were considered. On average, 94% of the pixels inside the basin were used, varying from 60% in February (rainy season) to 100% in drier seasons. Our results show that, even after different levels of BRDF correction, EVI_{NBAR} and EVI_{SAR} still reveal clear seasonal patterns. This result contrasts with *Morton et al.* [2014], who showed that greening patterns during the dry season could not be observed after BRDF correction. The discrepancy could be explained by the use of different BRDF correction methods or may represent genuine seasonal vegetation changes.

Interestingly, the only difference between the EVI_{NBAR} and the EVI_{SAR} data sets is the monthly average Sun zenith angle considered in the BRDF model. While in the EVI_{NBAR} Sun zenith angle corresponds to the angle at local solar noon, in the EVI_{SAR} the angle is fixed to 30°. The use of a constant Sun zenith angle causes an evident smoothing in the seasonal variation of EVI_{SAR}, indicating that Sun-sensor geometry is in part responsible for intra-annual patterns (Figure 3d). Furthermore, we show that even after BRDF correction carried out in the EVI_{NBAR} and EVI_{SAR}, the seasonal pattern in these data sets still have a significant (p value < 0.001) correlation with monthly average phase angle (obtained from the MOD13 product). Hence, it is plausible that the BRDF model behind the EVI_{NBAR} and EVI_{SAR} cannot fully remove artifacts associated with Sun-sensor geometry, although genuine vegetation trend cannot be discarded. In agreement with *Galvão et al.* [2011], we observed that EVI_{SAR} is linearly correlated with BRDF-corrected NIR reflectance (Figure S6). On the other hand, red and blue bands show no correlation with EVI_{SAR}, leading to the conclusion that the remaining seasonal patterns are mainly driven by changes in NIR reflectance, which is not considered a good indicator of photosynthetic activity.

We also show that long-term monthly EVI_{SAR} averages are not significantly correlated with incoming radiation flux (Figure 3a). Monthly rainfall averages, on the other hand, show a significant correlation with EVI_{SAR} (p value < 0.05) (Figure 3b). However, this correlation does not necessarily represent causality, given that a significant relationship between EVI_{SAR} and rainfall is not observed when analyzing geographical areas with different rainfall patterns (see Figure S7). This statement is reinforced by the lack of EVI_{SAR} sensitivity to rainfall anomalies (showed in Figure 1). The seasonal patterns in the EVI_{NBAR} and EVI_{SAR} were consistent in all years from 2001 to 2012 (Figure S9).

Hence, we demonstrate that radiation and rainfall are unlikely to exert significant influence on EVI_{SAR} anomalies or long-term seasonal patterns. Moreover, we show that, after BRDF correction, seasonal variations are still evident in EVI_{SAR} data set. However, can the seasonal pattern found in EVI_{SAR} help quantify changes in Amazon forest productivity? To answer this question, we compare monthly EVI_{SAR} with average GPP estimates based on eddy covariance [*Hutyra et al.*, 2007] (Figure 4). We also analyze ground measurements of rainfall and net radiation collected at the flux tower location [*Hutyra et al.*, 2007].

When comparing GPP (or NEE, or R_{eco}) to EVI, we must consider the different spatial footprints and temporal sampling strategies of these data. The footprint of the NEE (and thus GPP and R_{eco}) as measured by the K67 tower-based eddy covariance systems is likely to cover areas up to 3 km^2 in terms of daytime fluxes, with a smaller proportion of fluxes originating from areas as large as 70–80 km^2 [*Araújo et al.*, 2002]. Similarly, the temporal sampling strategy is different as NEE is measured continuously while EVI is constructed from disjunct satellite overpasses. However, if we assume both eddy covariance NEE and satellite EVI to be useful

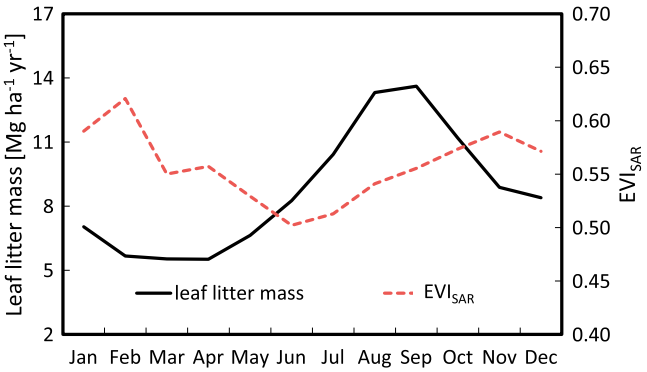

Figure 5. Monthly average leaf litterfall rate in the surrounding of the flux tower for the period July 2000 to May 2005 [*Rice et al*., 2008] and monthly average EVI_{SAR}.

products describing the general behavior of the forest in monthly time scales, the comparison of the temporal variations of these data could reveal potential correlations and connections.

GPP refers to gross canopy carbon dioxide uptake through photosynthesis, which can be estimated using measurements of net ecosystem exchange of CO_2 (NEE). NEE is the balance between GPP and ecosystem respiration (R_{eco}), $NEE = R_{eco} - GPP$. Here GPP and R_{eco} are always positive, and positive NEE indicates the ecosystem to be a source of CO_2 into the atmosphere, while negative NEE indicates the ecosystem to be a sink of CO_2. R_{eco} is typically estimated using nighttime measurements of NEE. For the description of the NEE data and partitioning to GPP and R_{eco}, see *Hutyra et al*. [2007]. NEE seasonal patterns are, therefore, intrinsically driven by a balance between GPP and R_{eco}. It is observed that NEE, GPP, and R_{eco} closely follow regional climate patterns (Figure 4). NEE shows positive values (indicating the forest is a source of carbon into the atmosphere) during the entire rainy season, a period in which photosynthetically active radiation is reduced due to higher cloud incidence and in which moisture is high. Between September and November (dry season), radiation increases, moisture decreases, and NEE decreases to negative values (indicating the forest is a carbon sink). R_{eco} follows a similar pattern, with higher values during lower radiation periods with more rain, decreasing as radiation increases and rainfall decreases. *Hutyra et al*. [2007] argue that the reduction of R_{eco} in the dry season is likely associated to moisture limitations on heterotrophic respiration.

Despite uncertainties in the mechanisms defining GPP seasonality [*Restrepo-Coupe et al*., 2013; *Hutyra et al*., 2007], there is strong evidence that environmental factors play a major role in the intra-annual variation of GPP. As a result, GPP reaches a low peak between June and August and a high peak during October and November. This pattern is correlated with EVI_{SAR} (p value < 0.05). This is in agreement with results obtained by *Huete et al*. [2006] using a MODIS EVI data set without BRDF correction. However, we show evidences that the factors defining EVI_{SAR} seasonality in the equatorial Amazon may be detached from the factors defining GPP variability. Given the connections between radiation, rainfall, NEE, and R_{eco}, it is expected that radiation anomalies are associated with departures from GPP averages. However, EVI_{SAR} was shown to have no sensitivity to water input or radiation (Figure 1).

In general terms, EVI is function of canopy reflectance, which varies according to the optical properties of canopy components, canopy structure (e.g., leaf area index), and Sun-sensor geometry. Previous studies demonstrate that seasonal variations in forest carbon exchange are linked to changes in leaf turnover [*Rice et al*., 2004; *Hutyra et al*., 2007]. At the K67 flux tower location, peak litterfall rates are observed around August [*Rice et al*., 2008], and the flush of new leaves, with higher photosynthetic efficiency, is also reported to occur around the same period, August–October [*Rivera et al*., 2002]. New leaves tend to have higher reflectance and increased transmittance relative to old leaves [*Roberts et al*., 1998]. Therefore, forest albedo would be expected to increase as old leaves are replaced with new. Our results show that EVI_{SAR} does not follow this pattern (Figure 5). EVI_{SAR} values start decreasing after January, while litterfall rate starts increasing only after April. When EVI_{SAR} reaches lowest values in June, litterfall rates continue increasing until September. Therefore, it is unclear from our analysis how changes in canopy structure or chemical composition associated with changes in the amount of leaves are driving the remaining seasonal patterns in the EVI_{SAR} dataset.

Finally, given that the EVI_{SAR} sensitivity to radiation diverges from the relationship between EVI_{SAR} and GPP, and greening patterns do not follow changes in canopy structure associated with leaf litterfall rates, we find important inconsistencies in the relationship between MODIS EVI and GPP in the equatorial forest. This result suggests that model estimates of ecosystem productivity based on MODIS EVI [e.g., *Brando et al*., 2010; *Potter et al*., 2009; 2012] should be interpreted with caution.

4. Summary and Conclusions

Our results show evidences that, after removing artifacts caused by clouds, aerosols, and Sun-sensor geometry, radiation and rainfall extremes exert no influence on EVI anomalies. Furthermore, radiation and rainfall show no evident influence on long-term EVI patterns in intact equatorial forests. In agreement with previous findings, our results confirm that the annual EVI seasonality is in part explained by variation in Sun-sensor geometry. However, we show that after BRDF correction, seasonal patterns are still present in intact evergreen forests, contradicting previous claims that seasonal changes in greening patterns cannot be observed after accounting for Sun-sensor geometry artifacts.

Despite a statistical correlation between monthly averages of GPP and EVI_{SAR}, we found loose connections between the factors driving the seasonality of these two variables. Previous studies provide evidences that GPP seasonality is linked to changes in canopy structure and chemical composition variations as a response to climate patterns. On the other hand, we show that EVI_{SAR} variation has limited influence of environmental factors and is not correlated to leaf litterfall rates.

Studies related to remote sensing of Amazon forest phenology and climate extreme impacts on vegetation have sparkled parallel but often disconnected discussions during the past years. Our results create elements to reconcile these discussions. We demonstrate central factors affecting EVI seasonal cycles and the occurrence of greenness anomalies. Accounting for these factors leads to the conclusion that in the Amazon forest, the relationship between vegetation functioning and MODIS EVI should be treated with caution.

Acknowledgments

This study was funded by the Academy of Finland. The MODIS and TRMM data can be obtained through the online data pools from NASA Distributed Active Archive Center (DAAC). Radiation flux data were obtained from the NASA Langley Research Center Atmospheric Science Data Center.

Wolfgang Knorr thanks two anonymous reviewers for their assistance in evaluating this paper.

References

Anderson, L. O., Y. Malhi, L. E. Aragão, R. Ladle, E. Arai, N. Barbier, and O. Phillips (2010), Remote sensing detection of droughts in Amazonian forest canopies, *New Phytol.*, *187*, 733–750, doi:10.1111/j.1469-8137.2010.03355.x.

Aragão, L. E. O. C., B. Poulter, J. B. Barlow, L. O. Anderson, Y. Malhi, S. Saatchi, O. L. Phillips, and E. Gloor (2014), Environmental change and the carbon balance of Amazonian forests, *Biol. Rev.*, doi:10.1111/brv.12088.

Araújo, A. C., et al. (2002), Comparative measurements of carbon dioxide fluxes from two nearby towers in a central Amazonian rainforest: The Manaus LBA site, *J. Geophys. Res.*, *107*(D20), 8090, doi:10.1029/2001JD000676.

Asner, G. P., and A. Alencar (2010), Drought impacts on the Amazon forest: The remote sensing perspective, *New Phytol.*, *187*, 569–578, doi:10.1111/j.1469-8137.2010.03310.x.

Bradley, A. V., F. F. Gerard, N. Barbier, G. P. Weedon, L. O. Anderson, C. Huntingford, L. E. Aragao, P. Zelazowski, and E. Arai (2011), Relationships between phenology, radiation and precipitation in the Amazon region, *Global Change Biol.*, *17*, 2245–2260, doi:10.1111/j.1365-2486.2011.02405.x.

Brando, P. M., S. J. Goetz, A. Baccini, D. C. Nepstad, P. S. A. Beck, and M. C. Christman (2010), Seasonal and interannual variability of climate and vegetation indices across the Amazon, *Proc. Natl. Acad. Sci. U.S.A.*, *107*(33), 14,685–14,690, doi:10.1073/pnas.0908741107.

Galvão, L. S., J. R. Santos, D. A. Roberts, F. M. Breunig, M. Toomey, and Y. M. Moura (2011), On intra-annual EVI variability in the dry season of tropical forest: A case study with MODIS and hyperspectral data, *Remote Sens. Environ.*, *115*(9), 2350−2359, doi:10.1016/j.rse.2011.04.035.

Huete, A. R., K. Didan, Y. E. Shimabukuro, P. Ratana, S. R. Saleska, L. R. Hutyra, W. Yang, R. R. Nemani, and R. Myneni (2006), Amazon rainforests green-up with sunlight in dry season, *Geophys. Res. Lett.*, *33*, L06405, doi:10.1029/2005GL025583.

Hutyra, L. R., J. W. Munger, S. R. Saleska, E. Gottlieb, B. C. Daube, A. L. Dunn, D. F. Amaral, P. B. de Camargo, and S. C. Wofsy (2007), Seasonal controls on the exchange of carbon and water in an Amazonian rain forest, *J. Geophys. Res.*, *112*, G03008, doi:10.1029/2006JG000365.

Lewis, S. L., P. M. Brando, O. L. Phillips, G. M. F. van der Heijden, and D. Nepstad (2011), The 2010 Amazon drought, *Science*, *331*, 554, doi:10.1126/science.1200807.

Morton, D. C., J. Nagol, C. C. Carabajal, J. Rosette, M. Palace, B. D. Cook, E. F. Vermote, D. J. Harding, and P. R. North (2014), Amazon forests maintain consistent canopy structure and greenness during the dry season, *Nature*, *506*, 221–224, doi:10.1038/nature13006.

Moura, Y. M., L. S. Galvão, J. R. Dos Santos, D. A. Roberts, and F. M. Breunig (2012), Use of MISR/Terra data to study intra- and inter-annual EVI variations in the dry season of tropical forest, *Remote Sens. Environ.*, *127*, 260–270, doi:10.1016/j.rse.2012.09.013.

Myneni, R. B., et al. (2007), Large seasonal changes in leaf area of Amazon rainforests, *Proc. Natl. Acad. Sci. U.S.A.*, *104*, 4820–4823, doi:10.1073/pnas.0611338104.

Phillips, O. L., et al. (2010), Drought-mortality relationships for tropical forests, *New Phytol.*, *187*, 631–646, doi:10.1111/j.1469-8137.2010.03359.x.

Potter, C., et al. (2009), Terrestrial carbon sinks in the Brazilian Amazon and Cerrado region predicted from MODIS satellite data and ecosystem modelling, *Biogeosciences*, *6*, 937–945, doi:10.5194/bg-6-937-2009.

Potter, C., S. Klooster, and V. Genovese (2012), Net primary production of terrestrial ecosystems from 2000 to 2009, *Clim. Change*, *115*(2), 365–378, doi:10.1007/s10584-012-0460-2.

Restrepo-Coupe, N., et al. (2013), What drives the seasonality of photosynthesis across the Amazon basin? A cross-site analysis of eddy flux tower measurements from the Brasil flux network, *Agr. Forest. Meteorol.*, *182–183*, 128–144, doi:10.1016/j.agrformet.2013.04.031.

Rice, A. H., et al. (2004), Carbon balance and vegetation dynamics in an old-growth Amazonian forest, *Ecol. Appl.*, *14*(4), 55–71, doi:10.1890/02-6006.

Rice, A. H., E. P. Hammond, S. R. Saleska, L. Hutyra, M. Palace, M. Keller, P. B. de Carmargo, K. Portilho, D. Marques, and S. C. Wofsy (2008), LBA-ECO CD-10 Forest Litter Data for km 67 Tower Site, Tapajos National Forest, Oak Ridge National Laboratory Distributed Active Archive Center, Oak Ridge, Tenn., doi:10.3334/ORNLDAAC/862.

Rivera, G., S. Elliott, L. S. Caldas, G. Nicolossi, V. T. R. Coradin, and R. Borchert (2002), Increasing day-length induces spring flushing of tropical dry forest trees in the absence of rain, *Trees Struct. Funct.*, *16*(7), 445–456.

Roberts, D. A., B. N. Nelson, J. B. Adams, and F. Palmer (1998), Spectral changes with leaf aging in Amazon Caatinga, *Trees*, *12*, 315–325.

Saleska, S. R., K. Didan, A. R. Huete, and H. R. da Rocha (2007), Amazon forests green-up during 2005 drought, *Science*, *318*(5850), 612, doi:10.1126/science.1146663.

Samanta, A., S. Ganguly, H. Hashimoto, S. Devadiga, E. Vermote, Y. Knyazikhin, R. R. Nemani, and R. B. Myneni (2010), Amazon forests did not green-up during the 2005 drought, *Geophys. Res. Lett.*, *37*, L05401, doi:10.1029/2009GL042154.

Samanta, A., S. Ganguly, E. Vermote, R. R. Nemany, and R. B. Myneni (2012a), Why is remote sensing of Amazon forest greenness so challenging?, *Earth Interact.*, *16*, 1–14, doi:10.1175/2012EI440.1.

Samanta, A., Y. Knyazikhin, L. Xu, R. E. Dickinson, R. Fu, M. H. Costa, S. S. Saatchi, R. R. Nemani, and R. B. Myneni (2012b), Seasonal changes in leaf area of Amazon forests from leaf flushing and abscission, *J. Geophys. Res.*, *117*, G01015, doi:10.1029/2011JG001818.

Silva, F. B., et al. (2013), Large-scale heterogeneity of Amazonian phenology revealed from 26-year long AVHRR/NDVI time-series, *Environ. Res. Lett.*, *8*, 02401, doi:10.1088/1748-9326/8/2/024011.

Xu, L., A. Samanta, M. H. Costa, S. Ganguly, R. R. Nemani, and R. B. Myneni (2011), Widespread decline in greenness of Amazonian vegetation due to the 2010 drought, *Geophys. Res. Lett.*, *38*, L07402, doi:10.1029/2011GL046824.